Nonequilibrium information entropy approach to ternary fission of actinides

G. Röpke, J. B. Natowitz, and H. Pais

Phys. Rev. C **103**, L061601 — Published 2 June 2021

DOI: 10.1103/PhysRevC.103.L061601

A Non-equilibrium Information Entropy Approach to Ternary Fission of Actinides

G. Röpke[1],* J. B. Natowitz[2],† and H. Pais[3]‡
[1] *Institut für Physik, Universität Rostock, D-18051 Rostock, Germany.*
[2] *Cyclotron Institute, Texas A&M University, College Station, Texas 77843, USA.*
[3] *CFisUC, Department of Physics, University of Coimbra, 3004-516 Coimbra, Portugal.*

Ternary fission of actinides probes the state of the nucleus at scission. Light clusters are produced in space and time very close to the scission point. Within the non-equilibrium statistical operator method, a generalized Gibbs distribution is constructed from the information given by the observed yields of isotopes. Using this relevant statistical operator, yields are calculated taking excited states and continuum correlations into account, in accordance with the virial expansion of the equation of state. Clusters with mass number $A \leq 10$ are well described using the non-equilibrium generalizations of temperature and chemical potentials. Improving the virial expansion, in-medium effects may become of importance in determining the contribution of weakly bound states and continuum correlations to the intrinsic partition function. Yields of larger clusters, which fail to reach this quasi-equilibrium form of the relevant distribution, are described by nucleation kinetics, and a saddle-to-scission relaxation time of about 7000 fm/c is inferred. Light charged particle emission, described by reaction kinetics and virial expansions, may therefore be regarded as a very important tool to probe the non-equilibrium time evolution of actinide nuclei during fission.

PACS numbers: 21.65.-f, 21.60.Jz, 25.70.Pq, 26.60.Kp

Introduction. - Nuclear fission remains an exciting field of research [1]. In the last few decades, an amazing progress has been realized with respect to experimental investigations and phenomenology, as well as in theoretical treatments and microscopic modelling. Nevertheless, basic concepts are still open for discussion, and an "*ab initio*" many-body theory remains a challenge given our present understanding of quantum many-particle physics. For a recent review on studies of thermal neutron induced ($n_{\rm th}$,f), and spontaneous fission (sf) of actinides, as well as a discussion on open theoretical questions, the reader should refer to [2–6].

In this letter we focus on ternary fission which has been discussed extensively in the literature. See, e.g., [7–16] and further references within. We show that a many-body approach, taking continuum correlations such as ^{4}H, ^{5}He, etc., into account, improves the description of ternary fission as observed for different actinides. The virial expansion of the intrinsic partition function, well-known from equilibrium thermodynamics, can be generalized to the non-equilibrium case if the information entropy approach is used. Another new result is the extension to larger light charged particles ($2 < Z \leq 6$). Above $Z = 5$ a critical behavior is obtained which is described by nucleation kinetics.

From a phenomenological point of view, the fission process can be generally described via a picture in which the deforming nucleus, following a dynamic path, subject to fluctuations, evolves from its ground state shape and crosses the barrier or outer saddle where the nascent fission fragments are formed. The deformed dumbbell-like system, consisting of two main fragments and the connecting neck region, then evolves toward the scission point where the rupture occurs. Dissipative dynamics has been applied to describe a non-adiabatic, strongly overdamped evolution from the saddle point to scission, see [1, 6, 17–21], though a rigorous treatment of the scission process is still unavailable. The saddle-to-scission time is estimated as $\tau_{s\to s} \approx O(10^3 - 10^4)$ fm/c [21]. A value $\tau_{s\to s} = 6400$ fm/c was quoted in Ref. [16], and $\tau_{s\to s} \approx 10^3$ fm/c in [17]. As pointed out in Ref. [4], the fission time scale remains one of the most controversial and least understood quantities in fission, see also [22].

A better understanding of the fission dynamics requires data of different nature such as the mass and energy distributions of the two fission fragments, and the multiplicities of the emitted particles, which are primarily neutrons, and of γ-radiation. We will not review here the progress which has been achieved in the measurement and interpretation of the fission-fragment mass distribution [4, 23–30] but mention only the introduction of a temperature of about 1 MeV to describe experimental distributions [1, 28, 29]. Temperature-like parameters of the order of 1 MeV are used to analyze the prompt fission neutron spectra of different actinides [3, 31–33]. The analysis of prompt fission γ-ray spectra for actinides [34–39] also suggests a temperature-like parameter of the same order. The use of concepts of statistical physics such as temperature prove to be fruitful for a phenomenological approach to fission. However, temperature is strictly defined for systems in thermodynamic equilibrium, but a fissioning nucleus is a finite system, not in thermodynamic equilibrium. We show below that within a non-equilibrium approach a Lagrange parameter $\lambda_T(t)$ can be introduced which may be considered as the non-equilibrium generalization of temperature.

An interesting feature, which is directly associated

*Electronic address: gerd.roepke@uni-rostock.de
†Electronic address: natowitz@comp.tamu.edu
‡Electronic address: hpais@uc.pt

isotope	$R^{\mathrm{vir}}_{A,Z}(1.3)$	$^{233}\mathrm{U}(n_{\mathrm{th}},\mathrm{f})$	$^{235}\mathrm{U}(n_{\mathrm{th}},\mathrm{f})$	$^{239}\mathrm{Pu}(n_{\mathrm{th}},\mathrm{f})$	$^{241}\mathrm{Pu}(n_{\mathrm{th}},\mathrm{f})$	$^{248}\mathrm{Cm(sf)}$	$^{252}\mathrm{Cf(sf)}$
λ_T [MeV]	-	1.24177	1.21899	1.3097	1.1900	1.23234	1.25052
λ_n [MeV]	-	-3.52615	-3.2672	-3.46688	-3.02055	-2.92719	-3.1107
λ_p [MeV]	-	-15.8182	-16.458	-16.2212	-16.6619	-16.7798	-16.7538
^{1}n	-	560012	1.409e6	722940	1.8579e6	1.606e6	1.647e6
^{1}H	-	28.131	28.16	42.638	19.52	21.079	30.096
$^2\mathrm{H}^{\mathrm{obs}}$	-	41	50	69	42	50	63
^{2}H	0.973	40.986	49.76	68.632	41.563	49.533	61.579
$^3\mathrm{H}^{\mathrm{obs}}$	-	460	720	720	786	922	950
^{3}H	0.998	457.27	715.29	714.79	780.39	913.76	943.12
^{4}H	0.0876	2.7772	4.97	5.627	6.057	8.742	8.219
^{3}He	0.997	0.0124	0.0076	0.0235	0.00431	0.00645	0.00933
$^4\mathrm{He}^{\mathrm{obs}}$	-	10000	10000	10000	10000	10000	10000
^{4}He	1	8858.46	8706.1	8615.7	8556.9	8313.98	8454.0
^{5}He	0.689	1130.75	1289.04	1374.7	1439.0	1680.75	1540.9
$^6\mathrm{He}^{\mathrm{obs}}$	-	137	191	192	260	354	270
^{6}He	0.933	115.89	158.98	159.01	211.68	276.96	222.4
^{7}He	0.876	21.262	33.997	35.983	51.742	80.634	58.16
$Y^{\mathrm{obs}}_{^6\mathrm{He}}/Y^{\mathrm{final,vir}}_{^6\mathrm{He}}$	-	0.9989	0.9897	0.9846	0.9869	0.9899	0.9622
$^8\mathrm{He}^{\mathrm{obs}}$	-	3.6	8.2	8.8	15	24	25
^{8}He	0.971	3.4725	6.764	6.4095	12.481	21.280	13.32
^{9}He	0.255	0.047077	0.105	0.111	0.219	0.455	0.258
$Y^{\mathrm{obs}}_{^8\mathrm{He}}/Y^{\mathrm{final,vir}}_{^8\mathrm{He}}$	-	1.0229	1.1936	1.3496	1.1811	1.1042	1.8409
^{8}Be	1.07	5.7727	2.594	5.147	2.188	2.819	2.544

TABLE I: Lagrange parameters λ_i, observed yields $Y^{\mathrm{obs}}_{A,Z}$ (rows denoted with $^AZ^{\mathrm{obs}}$) [10, 13, 40], and primary yields $Y^{\mathrm{rel,vir}}_{A,Z}$ (rows denoted with ^AZ) for H and He nuclei from ternary fission of ^{233}U(n_{th},f), ^{235}U(n_{th},f), ^{239}Pu(n_{th},f), ^{241}Pu(n_{th},f), ^{248}Cm(sf), and ^{252}Cf(sf). The prefactor $R^{\mathrm{vir}}_{A,Z}(\lambda_T)$ at $\lambda_T = 1.3$ MeV, which represents the intrinsic partition function, is also given. In addition, two rows show the ratio of the observed yields compared to the final yields $Y^{\mathrm{final,vir}}_{^6\mathrm{He}} = Y^{\mathrm{rel,vir}}_{^6\mathrm{He}} + Y^{\mathrm{rel,vir}}_{^7\mathrm{He}}$ and $Y^{\mathrm{final,vir}}_{^8\mathrm{He}} = Y^{\mathrm{rel,vir}}_{^8\mathrm{He}} + Y^{\mathrm{rel,vir}}_{^9\mathrm{He}}$. Note that *vir* stands for virial approximation. Data for ^{252}Cf(sf) are calculated in [45]. In an analogous manner, calculations have been performed for the other actinides as shown in the Supplementary Material [41].

with the scission process, is the emission of light charged particles observed in ternary fission processes, see, e.g., [7–16, 40] and references within. A light cluster with mass number A and charge Z, most often ^{4}He, is emitted in a direction perpendicular to the symmetry axis defined by the two main fission fragments, which have mass numbers A_{FF} distributed near half that of the fissioning nucleus (mass number A_{CN}). Ternary fission yields of a series of light isotopes $\{A, Z\}$ and energies have been measured for different actinides. Sets of experimentally observed yields are available for ^{233}U(n_{th},f), ^{235}U(n_{th},f), ^{239}Pu(n_{th},f), ^{241}Pu(n_{th},f), ^{248}Cm(sf), and ^{252}Cf(sf), see Refs. [10, 11, 13, 40]. We denote the experimentally observed yields with the superscript "obs". Data for these observed yields $Y^{\mathrm{obs}}_{A,Z}$, normalized to the total observed experimental yield of $^4\mathrm{He}^{\mathrm{obs}}$ taken as 10000, are presented in Tab. I.

As known from α-decay studies, a mean-field approach like TDHFB has problems describing the formation of clusters. For ternary fission, parameterizations of the measured yields employing a statistical distribution with a temperature-like parameter $T \approx 1$ MeV, see [12–14], have been explored. However, any interpretation of the detected yields by a simple nuclear statistical equilibrium (NSE) model, see Eq. (4) below, faces some problems. The observed yields seen in the detector contain contributions from decaying excited states and resonances so that the observed yield distribution differs from the primary distribution at the time of scission. In addition, yields of light charged clusters with mass number $A \geq 10$ are clearly overestimated by the simple NSE distribution [13]. Modifications have been proposed [16] based on nucleation theory [42, 43]. Chemical equilibrium constants were recently derived [44] for the fission reaction ^{241}Pu(n_{th},f) accounting for in-medium effects. In Ref. [45], a non-equilibrium approach was used to discuss the observed yields of isotopes with $Z \leq 2$ for the spontaneous fission of ^{252}Cf. In this letter, we extend the non-equilibrium approach to other actinides and larger values of Z considering partial intrinsic partition functions including continuum contributions on the level of quantum virial expansions. We determine the non-equilibrium generalization of temperature and show that continuum correlations have to be included.

Non-equilibrium information entropy approach. - We describe fission as a non-equilibrium process, using the method of the non-equilibrium statistical operator (NSO), see [46–48]. The time evolution of a many-particle system, with Hamiltonian H, is described by the statistical operator $\rho(t)$. It is easily shown that

$$\rho(t) = \lim_{\epsilon\to 0} \epsilon \int_{-\infty}^{t} dt' e^{-\epsilon(t-t')} e^{-\frac{i}{\hbar}H(t-t')} \rho_{\rm rel}(t') e^{\frac{i}{\hbar}H(t-t')} \tag{1}$$

is a solution of the von Neumann equation with boundary conditions characterizing the state of the system in the past ($t' < t$), as expressed by the relevant statistical operator $\rho_{\rm rel}(t')$. The non-equilibrium state of the system is characterized by the averages of a set of observables $\{B_i\}$ denoted as relevant observables, examples are currents, occupation numbers, concentrations of reacting components, as well as by the densities of energy and particle numbers. The relevant statistical operator is constructed from known averages of relevant observables, using information theory. As it is well known from equilibrium statistical physics, the relevant distribution is determined from the maximum of information entropy $-{\rm Tr}\{\rho_{\rm rel}\ln[\rho_{\rm rel}]\}$ under given constraints,

$${\rm Tr}\{\rho_{\rm rel}(t')B_i\} = {\rm Tr}\{\rho(t')B_i\} \equiv \langle B_i\rangle^{t'}, \tag{2}$$

which are taken into account by Lagrange multipliers $\lambda_i(t')$. A minimum set of relevant observables consists of the conserved observables, i.e., energy H, and the numbers N_τ of neutrons and protons ($\tau = n, p$). The solution is the generalized Gibbs distribution

$$\rho_{\rm rel} = \frac{e^{-(H-\lambda_n N_n-\lambda_p N_p)/\lambda_T}}{{\rm Tr}\{e^{-(H-\lambda_n N_n-\lambda_p N_p)/\lambda_T}\}} \tag{3}$$

which physically corresponds to the most probable distribution under constraints on $\langle N\rangle^{t'}, \langle Z\rangle^{t'}$, and $\langle H\rangle^{t'}$. Note that these Lagrange multipliers λ_i, which are in general dependent on the parameter t', are not identical to the equilibrium parameters temperature T and chemical potentials μ_τ, but may be considered as non-equilibrium generalizations of the temperature and chemical potentials. In the limit of thermodynamic equilibrium, the information entropy can be identified with the thermodynamic entropy, and the Lagrange parameters λ_T, λ_τ can be identified with the thermodynamic variables T and μ_τ. Note that the NSO allows the possibility of including other relevant observables, such as the pair amplitude in the superfluid state, or the occupation numbers of the quasiparticle states to derive kinetic equations and to calculate reaction rates [47, 48].

As typical for a variational approach, we have to eliminate the Lagrange multipliers $\lambda_i(t')$ solving Eq. (2), in order for the constraints ${\rm Tr}\{\rho(t')B_i\}$ to be satisfied, see also [46]. For non-interacting systems, the equilibrium solutions are the well-known equations of state for ideal Fermi or Bose gases. For a Hamiltonian H containing nucleon-nucleon interactions, see [45], the evaluation of averages with $\rho_{\rm rel}$ (3), denoted here as relevant averages, leads to a many-particle problem which can be treated with the methods of quantum statistics. [Note that the mathematical concepts developed in equilibrium quantum statistics can also be used for the generalized Gibbs state $\rho_{\rm rel}$, Eq. (3).]

As shown in [49] and further references given there, the method of thermodynamic Green functions can be applied. A cluster expansion of the single-nucleon self-energy allows the introduction of partial densities of different clusters $\{A, Z\}$. These partial densities of clusters are denoted as relevant densities because they are calculated with the relevant statistical operator $\rho_{\rm rel}$ (3). The calculated yields which are proportional to the relevant densities are denoted by relevant yields $Y^{\rm rel}_{A,Z}$. As detailed in [49] and references given within, a virial expansion can be performed which leads, e.g., to a generalized Beth-Uhlenbeck formula [50, 51]. As a result, the relevant yields in the virial approximation are calculated as

$$Y^{\rm rel,vir}_{A,Z} \propto R^{\rm vir}_{A,Z}(\lambda_T)\, g_{A,Z} \left(\frac{2\pi\hbar^2}{Am\lambda_T}\right)^{-3/2} \times e^{(B_{A,Z}+(A-Z)\lambda_n+Z\lambda_p)/\lambda_T} \tag{4}$$

(nondegenerate limit), where $B_{A,Z}$ denotes the (ground state) binding energy and $g_{A,Z}$ the degeneracy [52]. The pre-factor

$$R^{\rm vir}_{A,Z}(\lambda_T) = 1 + \sum_i^{\rm exc} [g_{A,Z,i}/g_{A,Z}] e^{-E_{A,Z,i}/\lambda_T} \tag{5}$$

is related to the intrinsic partition function of the cluster $\{A, Z\}$. The summation is performed over all excited states of excitation energy $E_{A,Z,i}$ and degeneracy $g_{A,Z,i} = 2J_{A,Z,i} + 1$ [52], which decay to the ground state. Also, the continuum contributions are included in the virial expression. For instance, the Beth-Uhlenbeck formula expresses the contribution of the continuum to the intrinsic partition function via the scattering phase shifts, see [51, 53]. For $R^{\rm vir}_{A,Z}(\lambda_T) = 1$, the simple nuclear statistical equilibrium (NSE) is obtained, i.e., neglecting the contribution of all excited states including continuum correlations. Note that accounting for continuum states may diminish the value of $R^{\rm vir}_{A,Z}(\lambda_T)$, as is well known from the deuteron channel, see [49] and references therein.

In the low-density limit, virial expansions of the intrinsic partition functions of the channel $\{A, Z\}$ have been obtained [49, 51, 53] for ^{2}H, ^{4}H, ^{5}He, ^{8}Be using the measured phase shifts in the corresponding channels. The values are given in the second column of Tab. I for $\lambda_T = 1.3$ MeV. Well-bound states with energies far below the continuum edge so that excitation energy for continuum states is large compared to λ_T make only a weak continuum state contribution so that $R^{\rm vir}_{A,Z}(\lambda_T) \approx 1$, if no further excited states are present. An interpolation formula, which relates the pre-factor $R^{\rm vir}_{A,Z}(\lambda_T)$ to the energy of the edge of continuum, is given in [49], and the corresponding estimates of the pre-factor for the He isotopes with $6 \leq A \leq 9$ are also shown in Tab. I.

Within the NSO approach, Eq. (1), the relevant distribution $\rho_{\rm rel}$ serves as the initial condition to solve the von Neumann equation for $\rho(t)$. The evolution of the system happens according to the system Hamiltonian. The relevant (or primary) distribution $Y^{\rm rel}_{A,Z}(\lambda_T)$ contains stable and unstable states of nuclei, as well as correlations in the continuum (e.g., resonances).

The concept of introducing the relevant primary yield distribution according to the NSO is supported by several experimental observations. These include the observation of ^{5}He and ^{7}He emission [40] as well as the observed population of the 3.368 MeV first excited state of ^{10}Be [54], and the 2.26 MeV excited states of ^{8}Li [40]. Also of interest are the inferred data for ^{8}Be and $^7{\rm Li}_{7/2^-}$ observed in [55], which cannot be described with the NSE but demand a treatment with continuum states.

We used Lagrange parameters λ_i which are not time-dependent to infer the primary yield distribution. It is assumed that these parameters characterize the formation of clusters, and the cluster formation is established at scission. The subsequent evolution of the distribution is described by taking into account the decay of the excited states. The NSO approach includes also kinetic theory to describe this stage, see [46–48], but the derivation of reaction kinetics from first principles will not be considered in this work. Here, we approximate this process by the feeding of the final yields from the primary yields obtained from the relevant (or primary) distribution (4). For example, for $Z \leq 2$, the final yields are related to the primary, relevant yields as $Y^{\rm final}_{^3{\rm H}} = Y^{\rm rel}_{^3{\rm H}} + Y^{\rm rel}_{^4{\rm H}}$, $Y^{\rm final}_{^4{\rm He}} = Y^{\rm rel}_{^4{\rm He}} + Y^{\rm rel}_{^5{\rm He}} + 2Y^{\rm rel}_{^8{\rm Be}}$, $Y^{\rm final}_{^6{\rm He}} = Y^{\rm rel}_{^6{\rm He}} + Y^{\rm rel}_{^7{\rm He}}$, and $Y^{\rm final}_{^8{\rm He}} = Y^{\rm rel}_{^8{\rm He}} + Y^{\rm rel}_{^9{\rm He}}$.

In this work, to construct the relevant distribution $\rho_{\rm rel}$ from an information theoretical approach, we use the least squares method, see [16], to optimize the reproduction of the experimentally observed yields by the calculated final yields. We calculate the primary distribution $Y^{\rm rel,vir}_{A,Z}$ using the intrinsic partition function in the virial form, i.e. using the excited states and scattering phase shifts neglecting in-medium corrections. The optimum values of the Lagrange parameters λ_i are given in Tab. I for the different ternary fissioning actinides. While the dependence of λ_i from $\{A_{CN}, Z_{CN}\}$ of the parent actinide nucleus is a topic of interest [12, 14], the current accuracy of the experimental data is not sufficient to determine significant trends.

H *and* He *isotopes.* - The measured total yields of H and He isotopes are nearly perfectly reproduced by the corresponding sums of primary yields. The yield of ^{6}He is slightly overestimated by $Y^{\rm final,vir}_{^6{\rm He}}$. In contrast, the yield of ^{8}He is underestimated by $Y^{\rm final,vir}_{^8{\rm He}}$. Both ratios $Y^{\rm obs}_{^6{\rm He}}/Y^{\rm final,vir}_{^6{\rm He}}$ and $Y^{\rm obs}_{^8{\rm He}}/Y^{\rm final,vir}_{^8{\rm He}}$ are presented in Tab. I. Presently, the relevant distribution $Y^{\rm rel,vir}_{A,Z}$ does not take in-medium effects, in particular Pauli blocking, into account. Medium modifications are more effective for weakly bound clusters. As proposed in [45] for ^{252}Cf(sf), a stronger reduction of the yield of ^{6}He$^{\rm obs}$ compared to ^{8}He$^{\rm obs}$ may be related to the very low binding energy (0.975 MeV) of the ^{6}He nucleus below the $\alpha + 2n$ threshold. The suppression of ^{6}He$^{\rm obs}$ appears for all considered fissioning actinides and may be considered as a signature of the Pauli blocking. However, to address the problem, precise experimental data are needed. Experimental studies are still scarce, and the data are often not consistent [56, 57].

Unbound nuclei such as ^{5}He should be very sensitive to medium modifications. The virial expression for the intrinsic partition function is known [53], and the corresponding primary yields are given in Tab. I. Fortunately, in the case of ^{252}Cf, the primary yields of ^{5}He and ^{7}He have been measured [40], and the value $Y^{\rm obs}_{^5{\rm He}} = 1736(274)$ has been given there. In principle, because of the medium modifications, the different cluster states may serve as a probe to determine the neutron density in the neck region at scission, but the uncertainties are still rather large.

Isotopes with 2< Z ≤6. - A detailed measurement of the yields of ternary fission isotopes up to ^{30}Mg has been made for ^{241}Pu($n_{\rm th}$,f) [10, 11]. Extended sets of data for $Z > 2$ are also measured for ^{235}U($n_{\rm th}$,f) and ^{245}Cm($n_{\rm th}$,f) [11]. We have extended our analysis of the measured data up to $Z = 6$ using the relevant distribution, see [41] where these data are listed. In general, the neutron separation energy S_n, for each isotope, is adopted as the threshold energy for the continuum, but cluster decay is also possible, e.g., $^6{\rm Li} \to \alpha + d$, $^7{\rm Li} \to \alpha + t$, $^7{\rm Be} \to \alpha + h$, $^8{\rm Be} \to 2\alpha$, $^{10}{\rm B} \to \alpha + {^6{\rm Li}}$, etc. In some cases, such as ^{6}He, ^{8}He, ^{11}Li, two-neutron separation determines the threshold. To estimate the continuum correlation, the interpolation $R^{\rm vir}_{A,Z}(\lambda_T)$ [45] was used at the corresponding binding energy $E^{\rm thresh}_{AZ} - E_{A,Z,i}$ of the (ground state or excited) cluster. The final yields $Y^{\rm final,vir}_{A,Z}$ are calculated taking into account any modifications resulting from gains or losses occurring during the decay of the primary isotopes. A list of excited states of the isotopes with $2 < Z \leq 6$ and the corresponding intrinsic partition functions is given in [41].

The question arises whether global Lagrange parameters $\lambda_T, \lambda_n, \lambda_p$, which are valid for all Z exist, as expected for matter in thermodynamic equilibrium. Before we discuss this question, we present a calculation with the relevant distribution given above, employing only three Lagrange parameters λ_i, but taking also Li isotopes into account. A least squares fit of final yields $Y^{\rm final,vir}_{A,Z}$ to $Y^{\rm obs}_{A,Z}$ for ^{2}H, ^{3}H, ^{4}He, ^{8}He, ^{7}Li, ^{8}Li, ^{9}Li has been performed. The accuracy of the fit increases since, here, ^{6}He and ^{11}Li are not included. Both are weakly bound systems for which medium effects and dissolution may become of relevance, as discussed above. Again we emphasize that in-medium corrections are not included in the present calculation. The Lagrange parameter values $\hat{\lambda}_T = 1.2023$ MeV, $\hat{\lambda}_n = -2.9981$ MeV, $\hat{\lambda}_p = -16.6285$ MeV are obtained for ^{241}Pu($n_{\rm th}$,f). There are only minimal changes compared to those derived from the fit of Tab. I for ^{241}Pu($n_{\rm th}$,f), and we conclude that our approach can also reproduce the yields of isotopes with $Z = 3$.

Using these Lagrange parameter values $\hat{\lambda}_i$ and considering all observed data for isotopes with $Z \leq 6$, the ratio $Y^{\rm obs}_{A,Z}/Y^{\rm final,vir}_{A,Z}$ is shown as a function of the mass number A in Fig. 1. Surprisingly, yields of ^{9}Be, ^{10}Be, ^{11}B are also well reproduced. For $A \geq 11$, the calculations overestimate the observed yields, and the ratios decrease strongly, starting around $A = 10$.

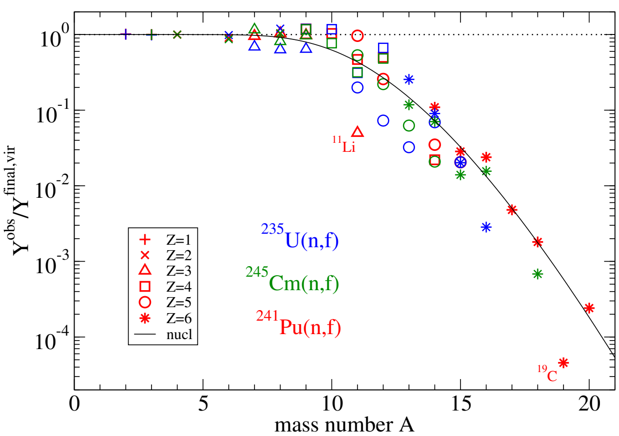

FIG. 1: (Color online) Ternary fission of ^{235}U($n_{\rm th}$,f) (blue), ^{245}Cm($n_{\rm th}$,f) (green), and ^{241}Pu($n_{\rm th}$,f) (red): Ratio $Y^{\rm obs}_{A,Z}/Y^{\rm final,vir}_{A,Z}$ as function of the mass number A. Isotopes with $Z \leq 6$ are shown. Black full line: Fit of nucleation kinetics (6) to the data of ^{241}Pu($n_{\rm th}$,f). For tables of the data shown in this figure see the Supplementary Material [41].

An explanation of the decrease has been given in [16] using nucleation theory [42, 43]. Whereas small clusters are already in a quasi-equilibrium distribution $Y^{\rm rel}_{A,Z}$, larger clusters need more formation time so that the observed yields are smaller than those predicted by the relevant distribution. From reaction kinetics, the expression

$$Y^{\rm obs}_{A,Z}/Y^{\rm final,vir}_{A,Z} = \frac{1}{2}{\rm erfc}\left[b(\tau)(A^{1/3} - a(A_c,\tau))\right] \qquad (6)$$

is obtained, see [16], where $b(\tau) = (27.59\,{\rm MeV}/\lambda_T)^{1/2} \times (1 - e^{-2\tau})^{-1/2}$ and $a(A_c,\tau) = A_c^{1/3}(1 - e^{-\tau}) + e^{-\tau}$. With $\lambda_T = 1.2$ MeV, the least squares fit to the data of ^{241}Pu($n_{\rm th}$,f) (black line in Fig. 1) gives $\tau = 1.5406$, $A_c = 16.143$. Then, $c\tau_{s\to s} = \tau A_c^{2/3}\lambda_T^{1/2}/(3.967\,\rho)$, and with $\rho = 4 \times 10^{-4}$ fm^{-3} [16] follows $\tau_{s\to s} = 6793$ fm/c. This time scale supports the slow evolution from saddle to scission proposed recently as a dissipative process [6, 21].

The strong reduction of isotopes $A > 10$ compared to estimates of a statistical model is also seen in [13]. In addition, the overestimate of ^{5}He is shown there. The correct treatment of continuum correlations proposed in this letter removes this discrepancy.

The yields of weakly bound clusters ^{11}Li, ^{19}C are strongly overestimated, see [58]. A reason may be the shift of the binding energy due to in-medium effects. If the density is larger than the Mott density, the bound states are dissolved. Bound states with threshold energies below or near 1 MeV include also ^{6}He, ^{11}Be, ^{14}Be, ^{14}B, ^{15}C. The yields of all these isotopes are overestimated. This may be considered as an indication of in-medium effects (Pauli blocking) leading to a shift and possibly the dissolution of the cluster. This possibility should be considered when more accurate data are available.

Conclusions - In conclusion, we describe the yields of light charged particles emitted from ternary fission of actinides by a non-equilibrium distribution based on many-particle theory. This quantum-statistical approach, which has been successfully worked out already for the nuclear matter equation of state, symmetry energy, and other equilibrium properties, can also be used to describe the evolution of systems in non-equilibrium. In particular, excited states and continuum correlations are taken into account on the level of virial expansions. A new result of our non-equilibrium information entropy approach is the correct description of unbound states, such as ^{4}H, ^{5}He, ^{8}Be, as continuum correlations. This improves former treatments using simple NSE approaches, see, e.g. [13], which lead to strong irregularities. For low-A isotopes, the ratio of observed yields to calculated yields exhibit smaller fluctuations after the correct intrinsic partition functions are incorporated, see Fig. 1. We have shown that above a critical cluster size of $A \approx 10$ deviations from the quasi-equilibrium are seen, which we interpreted as the result of nucleation kinetics. An interesting result is that light charged particle distributions of ternary fission of different actinides show similar behavior.

The investigation of ternary fission has the advantage that it is directly related to the scission process, and that it can be localized in the neck region. It is an outstanding signal to explore the fission process, and more consistent and accurate data are necessary to work out a complete description of the ternary fission process within non-equilibrium quantum statistics.

Acknowledgments

This work was supported by the United States Department of Energy under Grant # DE-FG03- 93ER40773, by the German Research Foundation (DFG), Grant # RO905/38-1, the FCT (Portugal) Projects No. UID/FIS/04564/2019 and UID/FIS/04564/2020, and POCI-01-0145-FEDER-029912, and by PHAROS COST Action CA16214. H. P. acknowledges the grant CEECIND/03092/2017 (FCT, Portugal).

[1] H. J. Krappe and K. Pomorski, *Theory of Nuclear Fission (Lecture Notes in Physics)*, vol. 383 (Springer, Heidelberg 2012).
[2] N. Schunck and L. M. Robledo, Rep. Prog. Phys. **79**, 116301 (2016).
[3] K.-H. Schmidt and B. Jurado, Rep. Prog. Phys. **81**, 106301 (2018).
[4] A. N. Andreyev, K. Nishio, and K.-H. Schmidt, Rep. Prog. Phys. **81**, 016301 (2018).
[5] M. Bender, R. Bernard, G. Bertsch, *et al.*, J. Phys. G: Nucl. Part. Phys. **47**, 113002 (2020).
[6] A. Bulgac, S. Jin, and I. Stetcu, Front. Phys. **8**, 63 (2020).
[7] C. Wagemans, in *The Nuclear Fission Process*, edited by C. Wagemans (CRS Press, Boca Raton, 1991), Chap.12.
[8] M. Mutterer and J. P. Theobald, *Nuclear Decay Modes*, edited by D. Poenary (IOP, Bristol, 1996), Chap. 12.
[9] *Nuclear Particle Correlations and Cluster Physics*, edited by W. U. Schröder (World Scientific, Singapore, 2017), Chaps. 2, 12, 13, 21.
[10] U. Koester, H. Faust, G. Fioni, T. Friedrichs, M. Gross, and S. Oberstedt, Nucl. Phys. A **652**, 371 (1999).
[11] U. Koester, *Ausbeuten und Spektroskopie radioaktiver Isotope bei LOHENGRIN und ISOLDE*, thesis work, Technische Universität München, 2000.
[12] M. N. Andronenko, L.N. Andronenko, W. Neubert, and D.M. Seliverstov, Eur. Phys. J. A **12**, 185 (2001).
[13] G. V. Val'skii, Yad. Fiz. **67**, 1288 (2004) [Sov. J. Nucl. Phys. **67**, 1264 (2004)].
[14] J. P. Lestone, Phys. Rev. C **72**, 014604 (2005).
[15] J. P. Lestone, Int. J. Mod. Phys. E **17**, 323 (2008).
[16] S. Wuenschel, H. Zheng, K. Hagel, B. Meyer, M. Barbui, E. J. Kim, G. Roepke, and J. B. Natowitz, Phys. Rev. C **90**, 011601(R) (2014).
[17] A. J. Sierk, Phys. Rev. C **96**, 034603 (2017).
[18] J. Randrup and P. Möller, Phys. Rev. Lett. **106**, 132503 (2011).
[19] J. Randrup, P. Möller, and A. J. Sierk, Phys. Rev. C **84**, 034613 (2011).
[20] M. R. Mumpower, P. Jaffke, M. Verriere, and J. Randrup, Phys. Rev. C **101**, 054607 (2020).
[21] A. Bulgac, S. Jin, K. J. Roche, N. Schunck, and I. Stetcu, Phys. Rev. C **100**, 034615 (2019).
[22] D. Jacquet and M. Morjean, Prog. Part. Nucl. Phys. **63**, 155 (2009).
[23] H. Goutte, J. F. Berger, P. Casoli, and D. Gogny, Phys. Rev. C **71**, 024316 (2005).
[24] C. Simenel, Phys. Rev. Lett. **105**, 192701 (2010).
[25] Physics D. Regnier, N. Dubray, N. Schunck, and M. Verriere, Phys. Rev. C **93**, 054611 (2016).
[26] D. Regnier, N. Dubray, and N. Schunck, Phys. Rev. C **99**, 024611 (2019).
[27] M. Verriere, N. Schunck, and T. Kawano, Phys. Rev. C **100**, 024612 (2019).
[28] J. Zhao, T. Niksic, D. Vretenar, and S.-G. Zhou, Phys. Rev. C **99**, 014618 (2019).
[29] J. Zhao, J. Xiang, Z.-P. Li, T. Niksic, D. Vretenar, and S.-G. Zhou, Phys. Rev. C **99**, 054613 (2019).
[30] P. Marevic and N. Schunck, Phys. Rev. Lett. **125**, 102504 (2020).
[31] M. Kocak, H Ahmadov, and G. Dere, Annals of Nuclear Energy **70**, 82 (2014).
[32] T. Granier, Physics Procedia **64**, 183 (2015).
[33] O. Iwamoto, J. Nucl. Sci. Technol. **45**, 910 (2008).
[34] D. Choudhury, A. Gatera, A. Gook, M. Lebois, A. Oberstedt, S. Oberstedt, L. Qi, and J. Wilson, AIP Conference Proceedings **2076**, 060002 (2019).
[35] A. Oberstedt, T. Belgya, R. Billnert, R. Borcea, T. Brys, W. Geerts, A. Gook, F.-J. Hambsch, Z. Kis, T. Martinez, S. Oberstedt, L. Szentmiklosi, K. Takacs, and M. Vidali, Phys. Rev. C **87**, 051602(R) (2013).
[36] A. Gatera, T. Belgya, W. Geerts, A. Gook, F.-J. Hambsch, M. Lebois, B. Maroti, A. Moens, A. Oberstedt, S. Oberstedt, F. Postelt, L. Qi, L. Szentmiklosi, G. Sibbens, D. Vanleeuw, M. Vidali, and F. Zeiser, Phys. Rev. C **95**, 064609 (2017).
[37] M. Lebois, J. N. Wilson, P. Halipre, A. Oberstedt, S. Oberstedt, P. Marini, C. Schmitt, S. J. Rose, S. Siem, M. Fallot, A. Porta, and A.-A. Zakari, Phys. Rev. C **92**, 034618 (2015).
[38] P. Talou, T. Kawano, M. B. Chadwick, D. Neudecker, and M. E Rising, J. Phys. G: Nucl. Part. Phys. **42**, 034025 (2015).
[39] H. Makii, K. Nishio, K. Hirose, R. Orlandi, R. Leguillon, T. Ogawa, T. Soldner, U. Koester, A. Pollitt, F.-J. Hambsch, I. Tsekhanovich, M. Ache, S. Czajkowski, L. Mathieu, C. M. Petrache, A. Astier, S. Guo, T. Ohtsuki, S. Sekimoto, K. Takamiya, R. J. W. Frost, and T. Kawano, Phys. Rev. C **100**, 044610 (2019).
[40] Yu. N. Kopatch, M. Mutterer, D. Schwalm, P. Thirolf, and F. Gönnenwein, Phys. Rev. C **65**, 044614 (2002).
[41] Supplementary Material to this work.
[42] J. Schmelzer, G. Ropke, and F.-P. Ludwig., Phys. Rev. C **55**, 1917 (1997).
[43] P. Demo and Z. Kozisek, J. Phys. G: Nucl. Part. Phys. **23**, 971 (1997).
[44] J. B. Natowitz, H. Pais, G. Ropke, J. Gauthier, K. Hagel, M. Barbui, and R. Wada, Phys. Rev. C **102**, 064621 (2020).
[45] G. Röpke, J.B. Natowitz, and H Pais, Eur. Phys. J. A **56**, 238 (2020).
[46] D. N. Zubarev, *Nonequilibrium Statistical Thermodynamics* (Plenum Press, New York 1974).
[47] D. N. Zubarev, V. Morozov, and G. Ropke, *Statistical Mechanics of Nonequilibrium Processes* (Akademie-Verlag/Wiley, Berlin 1997).
[48] G. Röpke, *Nonequilibrium Statistical Physics* (Wiley-VCH, Weinheim, 2013).
[49] G. Röpke, Phys. Rev. C **101**, 064310 (2020).
[50] G. Röpke, L. Münchow, and H. Schulz, Nucl. Phys. A **379**, 536 (1982); Phys. Lett. **B 110**, 21 (1982).
[51] M. Schmidt, G. Ropke, and H. Schulz, *Ann. Phys.* **202**, 57 (1990).
[52] Data tables of nuclei Nudat 2: https://www.nndc.bnl.gov/nudat2/
[53] C. J. Horowitz and A. Schwenk, Nucl. Phys. A **776**, 55 (2006).
[54] A. V. Daniel, G. M. Ter-Akopian, J. H. Hamilton, A. V. Ramayya, J. Kormicki, G. S. Popeko, A. S. Fomichev, A. M. Rodin, Yu. Ts. Oganessian, J. D. Cole, J. K. Hwang, Y. X. Luo, D. Fong, P. Gore, M. Jandel, J. Kliman, L. Krupa, J. O. Rasmussen, S. C. Wu, I. Y. Lee, M. A. Stoyer, R. Donangelo, and W. Greiner, Phys. Rev. C **69**,

041305(R) (2004).

[55] P. Jesinger, Yu. N. Kopatch, M. Mutterer, F. Gonnenwein, A. M. Gagarski, J. v. Kalben, V. Nesvizhevsky, G. A. Petrov, W. H. Trzaska, and H. -J. Wollersheim, Eur. Phys. J. A **24**, 379 (2005).

[56] M. Mutterer, Yu. N. Kopatch, S. R. Yamaledtinov, V. G. Lyapin, J. von Kalben, S. V. Khlebnikov, M. Sillanpaa, G. P. Tyurin, and W. H. Trzaska, Phys. Rev. C **78**, 064616 (2008).

[57] S. Vermote, Nucl. Phys. A **837**,176 (2010).

[58] U. Koester, H. Faust, T. Friedrichs, S. Oberstedt, G. Fioni, M. Gross, and I. Ahmad, Proceedings from the Pont d'Oye IV Conference, October 6-8, 1999, Habay-la-Neuve, Belgium.